JOURNAL OF CHEMICAL INFORMATION AND MODELING

Article

pubs.acs.org/jcim

The Effect of Membrane Environment on Surfactant Protein C Stability Studied by Constant-pH Molecular Dynamics

Catarina A. Carvalheda,[†] Sara R. R. Campos,* and António M. Baptista*

Instituto de Tecnologia Química e Biológica António Xavier, Universidade Nova de Lisboa, Av. da República, 2780-157 Oeiras, Portugal

Supporting Information

ABSTRACT: Pulmonary surfactant protein C (SP-C) is a small peptide with two covalently linked fatty acyl chains that plays a crucial role in the formation and stabilization of the pulmonary surfactant reservoirs during the compression and expansion steps of the respiratory cycle. Although its function is known to be tightly related to its highly hydrophobic character and key interactions maintained with specific lipid components, much is left to understand about its molecular mechanism of action. Also, although it adopts a mainly helical structure while associated with the membrane, factors as pH variation and deacylation have been shown to affect its stability and function. In this work, the conformational behavior of both the acylated and deacylated SP-C isoforms was studied in a DPPC bilayer under different pH conditions using constant-pH molecular dynamics simulations. Our findings show that both protein isoforms are remarkably stable over the studied pH range, even though the acylated isoform exhibits a labile helix−turn−helix motif rarely observed in the other isoform. We estimate similar tilt angles for the two isoforms over the studied pH range, with a generally higher degree of internalization of the basic N-terminal residues in the deacylated case, and observe and discuss some protonation−conformation coupling effects. Both isoforms establish contacts with the surrounding lipid molecules (preferentially with the *sn*-2 ester bonds) and have a local effect on the conformational behavior of the surrounding lipid molecules, the latter being more pronounced for acylated SP-C.

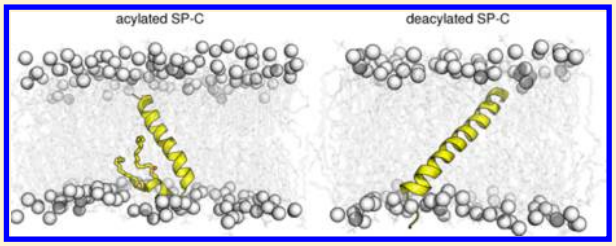

1. INTRODUCTION

The pulmonary surfactant is a complex mixture of phospholipids (∼40% dipalmitoylphosphatidylcholine, ∼30% unsaturated phosphatidylcholine, and ∼10% phosphatidylglycerol), neutral lipids (mainly cholesterol, ∼10%), and proteins (∼10%)[1] that delimits the alveolar surface, creating an air/water monolayer interface in the lungs that is repeatedly expanded (inhalation) and compressed (exhalation) during the breathing cycle.[2] When compressed, the surfactant film folds into the alveolar aqueous subphase, forming surfactant multilayer reservoirs through the exclusion of surfactant material from the air/water interface, which decreases the elastic recoil and prevents collapse of the alveolar system due to the increase in the surface pressure. This excluded material is then reincorporated into the interface during the spreading of the surface film when inspiration takes place, lowering the surface tension and reducing the energy required to inflate the lungs.[1,3,4]

Lung surfactant protein C (SP-C) is synthesized in the type-II pneumocyte cells of the alveolar wall, being translated into a proprotein that is cleaved and acylated during its transport toward the air/water interface.[5−7] Human mature SP-C is a short and highly hydrophobic polypeptide containing 35 amino acids with a highly conserved transmembrane helix region and a less conserved disordered, positively charged N-terminal segment containing two acylated cysteines flanked by prolines.[6,8−10] This protein was shown to be particularly important in promoting the stability of the alveolar interfacial film, facilitating the formation of interface-associated multilayer surfactant reservoirs upon alveolar compression and the reincorporation of the excluded material upon alveolar expansion.[3,11−13]

SP-C function is tightly related to its highly hydrophobic character and key interactions maintained with specific surfactant lipid components,[2,14] with the presence of the acyl chains seemingly enabling the protein to link the air/water interface to an adjacent bilayer or to link two bilayers together in the multilayer surfactant reservoirs.[2,7,15] SP-C has also been suggested to be important for maintaining lung function during oxygen injury, alveolar instability, and alveolar collapse;[7] its deficiency is associated with severe chronic respiratory dysfunctions over the long term,[16] and mutations in its encoding gene are linked to chronic lung disease.[17] In addition, its misfolding and aggregation are associated with pulmonary alveolar proteinosis,[18−20] an amyloid disease characterized by the accumulation of surfactant material in the alveolar space.

Several factors have been found to affect the conformational behavior of SP-C. Exposure to a nonmembrane environment,[21] deacylation,[22−24] and pH variations[25,26] were shown to

Received: February 9, 2015
Published: September 23, 2015

DOI: 10.1021/acs.jcim.5b00076
J. Chem. Inf. Model. 2015, 55, 2206−2217

destabilize the helix region and may contribute to the protein misfolding. While deacylation may be a consequence of the labile nature of the thioester-linked acyl chains,[27,28] pH variations are likely to occur during periods of disease, hypo- or hyperventilation, formation of tumors or abscesses, and physical disruption of the alveolar−capillary barrier.[29] Moreover, alveolar macrophages constitute a significant volume of the alveolar subphase and can be a substantial source of H^+ when metabolically active during inflammation and immune response.[29] However, the alveolar subphase was shown to be insensitive to pH changes in the blood, and its buffering capacity has never been quantified.[29]

Despite the considerable amount of biophysical data on SP-C, its extrapolation to a physiologically relevant environment is not always straightforward because of the use of diluted and/or simplified surfactant preparations and organic solvents known to compromise its structural stability and promote aggregation.[26,30] This is further complicated by the lack of structural data in membrane environments, although some coarse-grained studies have included SP-C in model surfactant membranes.[31−33]

The lack of detailed structural information in a physiological environment is one of the major factors hindering a better understanding of SP-C pathophysiology, a problem that may be tackled by performing atomistic simulations in membrane models. Until recently, the few works reporting atomistic molecular dynamics (MD) simulations of SP-C had been performed in pure solvents (chloroform, methanol, or water).[34−36] This led us to study SP-C in a chloroform/methanol/water mixture often used to mimic the membrane environment by means of constant-pH MD simulations,[26] which were intended to investigate the effects of pH and deacylation on the protein conformational behavior. Although the conclusions of this study were in line with the experimental observations that deacylation and nonacidic pH conditions destabilize the protein structure and lead to loss of helical content, we observed that this was related to the formation of pH-mediated intraprotein interactions favored by the low dielectric of the organic mixture and its limited membrane-mimetic character. This pointed out that considering a real lipid environment is essential for understanding SP-C function in vivo.

Here we present a constant-pH MD study where both the acylated and deacylated SP-C isoforms were studied under six different pH conditions (in the range 3 to 8) in a lipid bilayer. The stochastic titration method[37−41] was used, which can properly model the protonation−conformation coupling events in large systems, making it a suitable tool to capture key ionization-dependent protein−lipid interactions that are thought to be essential for the role of the protein in lung mechanics and disease. We focused on the conformational behavior of SP-C when it is inserted in a pure dipalmitoylphosphatidylcholine (DPPC) bilayer membrane, mimicking the molecular environment of the surfactant reservoirs in the alveolar subphase. DPPC is the major surfactant component and the one that most determines the surfactant tensoactive properties, making it a good model system to gain insights into the effects of pH and acylation on the ability of the protein to influence the lipid packing and the surfactant film stability. Some of the subjects that have been extensively discussed in the SP-C literature are addressed here in the context of a membrane bilayer environment, including (i) the role of SP-C charged residues on the protein function,[42−48] (ii) the effect of pH variations on the protein stability and structural behavior,[25,44,46,49,50] and (iii) the role of the protein acyl groups and key protein−lipid interactions in ensuring the membrane stability.[2,14,15,51] We also examine and discuss the orientation of the protein isoforms and how their presence affects some membrane properties.

2. MATERIALS AND METHODS

2.1. Surfactant Protein C Structure. The initial structures used in this work were the same as in ref 26 (Figure S1 in the Supporting Information). The starting-point structure was pig acylated SP-C (PDB code 1SPF)[9] mutated at five positions using PyMOL[52] to obtain the human sequence.[6] For the simulations with the acylated isoform, both cysteines (residues 5 and 6) were palmitoylated using PyMOL, and the force field parameters for the palmitoyl groups were adapted[26] from the D6PC building block in the GROMOS 45A3 force field.[53]

From the 20 available entries in the PDB file, five were chosen for use as initial structures for each isoform. However, during the equilibration phase (see section 2.3), only one of the acylated structures had both acyl chains properly accommodated in the membrane bilayer, and therefore, we decided to use only this one to perform the five constant-pH MD simulations.

2.2. MM/MD Settings. All of the molecular mechanics (MM)/MD simulations were performed using version 4.0.7 of the GROMACS package.[54,55] In order to ensure a liquid-crystalline-like phase, the temperature was kept at 323 K (since the DPPC phase transition temperature is 314.4 K[56,57]) using the v-rescale thermostat[58] with separate couplings for the protein, the lipids, and the water molecules and a time constant of 0.1 ps, unless indicated otherwise. The pressure was kept constant at 1 atm using the Berendsen barostat[59] with a time constant of 5 ps, unless indicated otherwise, and an isothermal compressibility of 4.6×10^{-5} bar^{-1}.[60,61]

In all of the MM/MD simulations, periodic boundary conditions were considered. The neighbor list was updated every five simulation steps (10 fs). The Coulombic interactions were treated with the reaction field approach[62] in the minimization/equilibration phases, while the generalized reaction field approach[63] was used in the MD steps of the constant-pH MD runs, applying a dielectric constant of 62[60,61] and an ionic strength of 150 mM. The nonbonded interactions were treated with the neighbor searching approach using a twin-range method with a lower cutoff of 0.8 nm and an upper cutoff of 1.4 nm, beyond which the van der Waals interactions were neglected.

All of the bonds were constrained using the LINCS algorithm.[64]

The GROMOS96 54A7 force field[65] was used, but the particular parameters for the DPPC molecules were the ones distributed by Poger et al.[60] in the Lipidbook repository.[66]

2.3. DPPC Bilayer Setup and System Preparation. Two bilayer systems containing 128 and 196 DPPC molecules were equilibrated to be used with the deacylated and acylated SP-C isoforms, respectively. In both cases, a pre-equilibrated lipid bilayer system of 128 DPPC molecules, distributed by Poger et al.[60] in the Lipidbook repository,[66] was used as a starting structure; in the latter case, this structure was replicated in order to obtain a 196 DPPC bilayer. The systems were respectively hydrated with 5841 and 9760 water molecules in a tetragonal box with periodic boundary conditions using the simple point-charge water model.[67]

DOI: 10.1021/acs.jcim.5b00076
J. Chem. Inf. Model. 2015, 55, 2206−2217

The system with 128 DPPC molecules was directly equilibrated during 100 ns of MD in the *NPT* ensemble, while the 196 DPPC system was first energy-minimized with 10^3 steps of steepest descent followed by 10^3 steps of low-memory Broyden−Fletcher−Goldfarb−Shanno (L-BFGS)[68] and then equilibrated in two MD steps, the first consisting of 100 ps in the *NVT* ensemble with a temperature time constant of 0.01 ps and the second consisting of 100 ns in the *NPT* ensemble with a temperature time constant of 0.1 ps. Some lipid properties were evaluated during the equilibration procedure to ensure a liquid-crystalline-like phase.

Five different initial structures for both the acylated and deacylated isoforms were inserted into the respective equilibrated bilayers using the methodology proposed by Schmidt and Kandt.[69] However, only one initial system was selected to perform the acylated isoform simulations after it was observed that the others did not properly accommodate the acyl chains in the membrane bilayer during the equilibration phase. This resulted in a set of five initial systems for the deacylated isoform and one initial system for the acylated isoform, the former containing 123−125 DPPC molecules and 7441−7475 water molecules and the latter 193 DPPC molecules and 11 375 water molecules. The systems were then energy-minimized with 10^3 steps of steepest descent with position restraints for the protein and DPPC atoms (100 and 1000 kJ mol^{-1} nm^{-2}, respectively) followed by 10^3 steps of steepest descent with position restraints for the protein atoms (100 kJ mol^{-1} nm^{-2}) and 10^3 steps of L-BFGS without position restraints. The equilibration phase was composed of three MD steps: 50 ps in the *NVT* ensemble with a temperature time constant of 0.01 ps and position restraints for the protein and DPPC atoms (1000 kJ mol^{-1} nm^{-2}); 100 ps in the *NPT* ensemble with a temperature time constant of 0.1 ps, a pressure time constant of 0.5 ps, and position restraints for the protein C_α atoms (1000 kJ mol^{-1} nm^{-2}) and the lipid atoms (100 kJ mol^{-1} nm^{-2}); and 150 ps in the *NPT* ensemble with a temperature time constant of 0.1 ps, a pressure time constant of 5 ps, and no position restraints. In the case of acylated SP-C, five replicates were generated by randomly selecting different sets of initial velocities from a Maxwell−Boltzmann distribution.

2.4. Constant-pH MD Simulations. Each equilibrated system was then simulated at six different pH values (3, 4, 5, 6, 7, and 8) for 100 ns using the stochastic titration method[37−41] for constant-pH MD. This method consists of a cycle with three steps: (1) a Poisson−Boltzmann/Monte Carlo (PB/MC) step that computes protonation free energy changes for a specific protein conformation at a given pH and assigns the new protonation states according to the last MC move; (2) an MM/MD segment in which the protein and the membrane are kept rigid, allowing the solvent molecules to adapt to the new charge configuration, here taken as 0.1 ps long;[41] and (3) an MM/MD segment of the whole unconstrained system, here taken as 10 ps long,[41] that samples the conformational space for the selected protonation state and whose last sampled conformation is used for a new PB/MC calculation in the following cycle. Although the stochastic titration method has been mostly used for proteins and peptides in solution,[70−74] it was recently extended to address membrane systems as well.[41,75] Since the rationale of the method is that a PB model can capture the energetics of (de)protonation changes in an "instantaneously frozen" molecular system immersed in a reorganizable solvent,[37] the lipid membrane is simply regarded as being part of that "frozen" system and treated accordingly. The reduced titration approach[38] was used to reduce the computational cost. Every 50 cycles, a complete titration was performed and the titratable sites list updated, considering an exclusion threshold of 0.999 relative frequency in a given state. The MM/MD settings were described in section 2.2, and the PB/MC settings are described below.

2.5. PB/MC Settings. The PB-derived free energy terms were calculated using version 2.2.9 of the MEAD package.[76] The atomic charges and radii were derived from the GROMOS 54A7 force field as described elsewhere,[77] with each atomic radius taken as half of the distance between that atom and a water molecule corresponding to a Lennard-Jones energy equal to $2RT$ above the minimum; these radii were found to yield good results in linear-response approximation (LRA) and constant-pH MD simulations of soluble peptides/proteins[26,38,39,70−74,78,79] and more recently also of a membrane-interacting peptide[41] and lipid bilayers.[75] The molecular surface was defined with a solvent probe of radius 1.4 Å and a Stern layer of 2.0 Å. The temperature was set to 323 K, the ionic strength to 150 mM, and the dielectric constant to 80 for the solvent and 2 for the protein and membrane bilayer. A two-step focusing procedure[80] was employed using grid spacings of 1.0 and 0.25 Å. The pK_a values for the model compounds in water, pK_{mod}, are given elsewhere.[26,81] The protonation states were sampled by MC simulations using the program PETIT,[82] performing 10^5 MC steps for each calculation. Each step consisted of a cycle of random choices of state (including tautomeric forms) for all of the individual sites and for pairs of sites with couplings above 2.0 pK_a units[82,83] whose acceptance/rejection followed a Metropolis criterion.[84]

We considered five titratable sites in the deacylated isoform (N-terminal amine, C5 and C6 thiols, H9 imidazole, and C-terminal carboxyl) and three titratable residues in the acylated isoforms (N-terminal, H9, and C-terminal). The K11 side-chain amine and the R12 guanidinium were considered to be always protonated. While the pK_a of Lys may shift down to ∼7 when Lys is constrained in the middle region of a transmembrane helix,[85,86] in SP-C it is located in the polar membrane region or water interface (see sections 3.3 and 3.4), hence easily stabilizing its charged form. In contrast, Arg is extremely difficult to neutralize[87] and retains its charged state even when placed in a similarly constrained transmembrane position.[85]

2.6. Analyses. All of the analyses were performed using GROMACS software or in-house tools, except the area per lipid and bilayer thickness, which were analyzed using APL@Voro.[88] For the average protein properties and lipid bilayer analysis, only the contribution of the equilibrated system was taken into account (after 25 ns of simulation time, based on different protein properties). The protein secondary structure was assigned using the DSSP criterion defined by Kabsch and Sander.[89] The root-mean-square fluctuation (rmsf) for each amino acid residue was determined after a C_α least-squares fit of all of the structures to the helical region of a central structure.[90] The protein tilt angle was defined as the angle between the protein helix first principal axis[91] and the coordinate z axis (i.e., the membrane normal), considering that the helix transmembrane region comprises residues 14−34 in the acylated isoform and residues 11−32 in the deacylated isoform. All of the presented molecular representations were created using PyMOL. Unless otherwise stated, errors were computed using standard correlation-correcting algorithms,[92] and the within-

DOI: 10.1021/acs.jcim.5b00076
J. Chem. Inf. Model. 2015, 55, 2206−2217

and across-replicates errors were combined using the law of total variance.[93]

The titration curves were obtained by averaging at each pH value the occupancy states of the titratable sites over the five final equilibrated segments.[39] A Hill curve, $f(\mathrm{pH}) = [1 + 10^{n(\mathrm{pH}-\mathrm{p}K_a)}]^{-1}$, where n represents the Hill coefficient, was fitted to the data using the nonlinear least-squares Marquardt–Levenberg algorithm[68] implemented in gnuplot 4.0.[94] In previous studies,[26,39,70,72] we performed these fits using the errors of the average occupancy at each pH value (obtained as indicated in the previous paragraph), taking the resultant normal-asymptotic standard errors[68] as the errors of the fitted parameters $\mathrm{p}K_a$ and n. However, this assumes a symmetric normal distribution for each point, which is obviously impossible near full (de)protonation (since error bars could then extend below 0 or above 1), and thus excessively penalizes "inward" deviations of the fitted curve away from those bounds, sometimes noticeably biasing the fit. Therefore, we decided to perform the fit without accounting for the errors of the average occupancies, adopting instead a bootstrap method[95] to estimate the errors of the fit parameters: (1) at each pH value, we randomly sampled (with replacement) five new average occupancies from the original set of five values (one per simulation) and computed their pH-specific global average; (2) these global averages (one per pH) were used to perform the fit of the Hill equation; (3) steps 1 and 2 were repeated 1000 times, producing 1000 values for each parameter ($\mathrm{p}K_a$ and n); (4) the error of each parameter was computed as the standard deviation of its 1000 values. As is usually done in the bootstrap method,[95] this procedure was used only to estimate the errors of the parameters, while their values were simply computed using the original sample as indicated above.

3. RESULTS AND DISCUSSION

3.1. Helix Stability: pH and Deacylation Effects. The structure of the porcine SP-C acylated isoform obtained by two-dimensional NMR spectroscopy[9] was observed to have an α-helix region comprising residues 9–34, which corresponds to a helical content of 74%. However, disparate data on the helical contents of different SP-C isoforms have been reported in the literature[23,45,51,96–100] because of the use of different experimental techniques, conditions, and/or system environments (organic mixtures, bilayer and monolayer systems), with values ranging between 50 and 90% for the acylated isoform and between 52 and 86% for the deacylated isoform in bilayer systems at around pH 7. Although chemical removal of the acyl moieties was reported to result in a decrease in SP-C helical content in some studies,[22,23,97] Flach et al.[101] and more recently Roldan et al.[51] found similar helical contents for the two protein isoforms.

In this section we start by analyzing the effects of pH and deacylation on the SP-C secondary structure (Figure 1). Except at pH 7, where the helical contents of the acylated and deacylated isoforms differ by around 12%, there is no statistically significant difference between the isoforms (also see Figure S2), which is in agreement with the most recent findings by Roldan et al.[51] In that experimental study, both isoforms were estimated to have around 80% helical content, which is somewhat higher than what we observed in the majority of our simulations, especially for the acylated isoform at pH 7.

The stability of the protein isoforms in a DPPC bilayer is in clear contrast with our previous work using a membrane-mimetic solution,[26] where the loss of helical content was significant for both isoforms over the same pH range (3 to 8) and the acylated isoform showed a higher helical content. The different structural consequences of deacylation in organic solvents and lipid membranes are in line with experimental observations[97,99] and have been suggested to be an outcome of the formation of stabilizing protein–lipid and/or protein–water interactions in a membrane environment that are lacking in the membrane-mimetic solutions.[26,102] Also, no pH trend in the SP-C stability was observed in the present study, in contrast to what was previously observed in the lipid-mimetic mixture.[25,26]

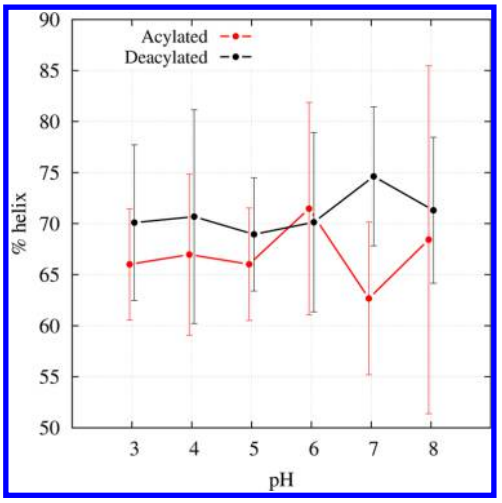

Figure 1. Percentages of helical content as functions of pH for the acylated (red line) and deacylated (black line) isoforms of SP-C in the DPPC bilayer. The percentage of helical content accounts for the contribution of the α-helix, 3-helix, and 5-helix motifs. For clarity of the error bars, the data for the acylated and deacylated forms are displaced by $\mp$0.04 pH units.

To understand the structural differences obtained for the two isoforms, the dominant secondary structural motifs were further analyzed at each pH (Figure 2). While the deacylated isoform presents a long and continuous helix region between residues 11 and 32, the acylated SP-C has a lower helicity in the N-terminal part, as the transmembrane helix region mostly comprises residues 14–34 (Figure 2, left). A distortion of the helix structure into turn motifs occurs, mainly between residues 6 and 10 in the deacylated isoform and between residues 5 and 12 of the acylated one, this behavior being generally more pronounced for the acylated isoform (Figure 2, right). The latter is also able to recover some helicity in this region, which leads to the formation of a labile helix–turn–helix motif in some simulations (Figure 3A,C and Figure S3). This distortion of the helix structure in the N-terminal region had already been predicted for the SP-C sequences of different species (including human) by Plasencia et al.,[103] and a helix–turn–helix conformation was earlier suggested by Johansson and Curstedt for the acylated isoform inserted in a bilayer lipid system.[102] The local perturbation of the helix structure introduced by the acylation of the cysteine residues at positions 5 and 6 is likely to arise from the structural restrictions imposed by the long acyl chains embedded in the bilayer interior, explaining the different conformational behavior observed for the two SP-C isoforms in our simulations. In contrast with the observations of Dluhy et al.[25] for a membrane-mimetic mixture, no β-sheet motifs were

DOI: 10.1021/acs.jcim.5b00076
J. Chem. Inf. Model. 2015, 55, 2206–2217

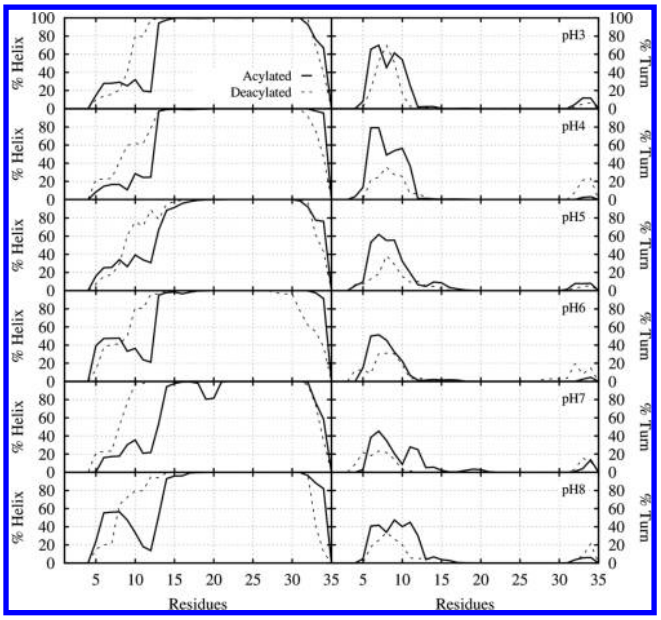

Figure 2. Percentages of time that each residue spends in the (left) helix and (right) turn conformations for the acylated (solid lines) and deacylated (dashed lines) isoforms of SP-C at different pH values in the DPPC bilayer, according to the DSSP criterion in use (see section 2.6).

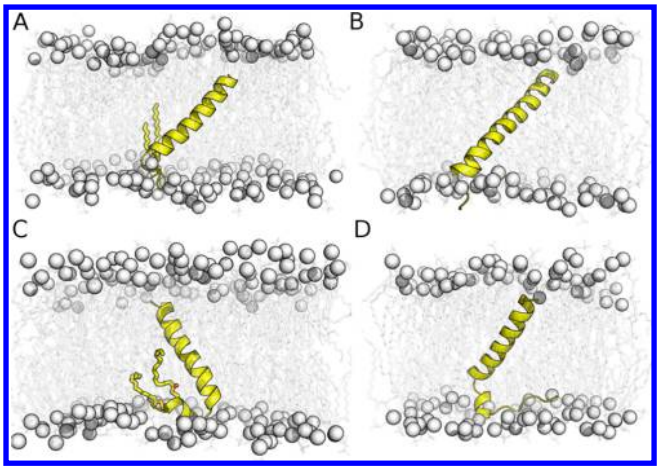

Figure 3. Cartoon representations of the common tilted conformations adopted by the (A, C) acylated and (B, D) deacylated SP-C isoforms in the DPPC bilayer. The protein can adopt a long and continuous helix transmembrane region (A, B) or exhibit a helix–turn–helix motif (C and D), which is more frequent in the acylated case. The protein is oriented with the N-terminus toward the bottom and the C-terminus toward the top.

observed in our simulations despite some loss of helical content.

We also analyzed the rmsf per residue over the studied pH range (Figure 4). Although the fluctuations observed for the acylated cysteines at positions 5 and 6 reflect a local increase of the N-terminal flexibility in the acylated isoform, the fluctuations of its transmembrane helix region are generally lower than the ones observed for the deacylated isoform. This means that although the acyl chains might cause a local distortion of the helix structure, they have a global effect in decreasing the protein flexibility. It is also noteworthy that in comparison with our previous work,[26] the helix rmsf's are

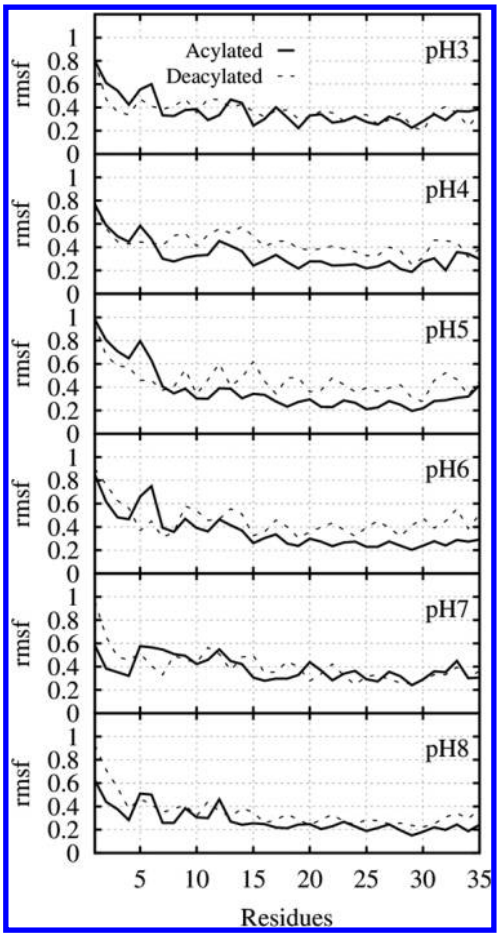

Figure 4. Root-mean-square-fluctuations (rmsf's) for each residue for the acylated (solid lines) and deacylated (dashed lines) isoforms of SP-C at different pH values in the DPPC bilayer.

considerably lower, which agrees well with the higher stability observed in the present study.

Taken together, the results in this section highlight the remarkable stability of both SP-C isoforms in a lipid environment and the structural effects of deacylation on the protein conformational behavior. Although it has a similar helical content, the acylated isoform exhibits a shortened transmembrane helix segment with a labile helix–turn–helix motif, which is rarely observed in the simulations of the deacylated isoform. This is in general agreement with experimental observations,[51,97,99] although the possibility of conformational changes that occur beyond the time scale simulated here cannot be ruled out. Furthermore, the contrasting results for the protein stability obtained in an organic solvent mixture[26] and the DPPC bilayer clearly show that a membrane environment is essential for understanding the effects taking part in the SP-C structure stabilization and the specific functions of SP-C in the lung surfactant film.

3.2. Protein Titration. To analyze the protein titration behavior of the acylated and deacylated SP-C isoforms, the average proton occupancies of the titratable sites at various pH values were used to compute the titration curves (Figure 5) and pK_a values (Table 1) (Hill coefficients and additional protonation data are given in Supporting Information). While the N-terminal residue (Nter) presents a pK_a that differs only slightly from the corresponding pK_{mod} value in both isoforms, the C-terminal residue (Cter) and H9 present significant shifts

DOI: 10.1021/acs.jcim.5b00076
J. Chem. Inf. Model. 2015, 55, 2206–2217

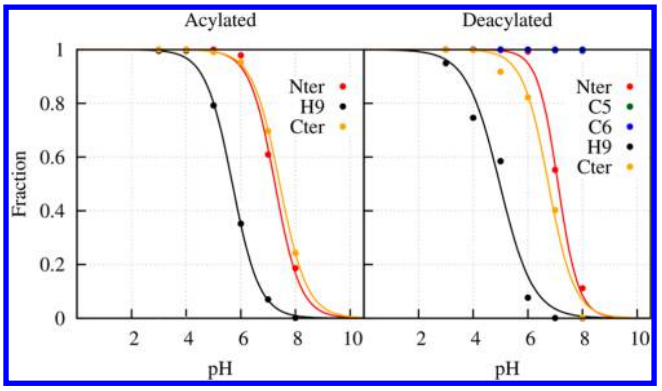

Figure 5. Titration curves for the sites considered titratable in the constant-pH MD simulations of the (left) acylated and (right) deacylated isoforms of SP-C in the DPPC bilayer. The sites Nter and Cter correspond to the N-terminal amine and C-terminal carboxyl groups, respectively. The points are average proton occupancies obtained from the simulations, and the lines are the corresponding Hill curve fits (see Materials and Methods). The errors in the average proton occupancies are shown in Figures S12 and S13.

Table 1. Computed pK_a Values for the Sites Considered Titratable in the Constant-pH MD Runs for the Acylated and Deacylated Isoforms in the DPPC Bilayer and the Respective pK_{mod} Values

	pK_a		
residue	acylated	deacylated	pK_{mod}
Nter	7.25 ± 0.21	7.10 ± 0.25	7.96
C5	–	>8	8.58
C6	–	>8	8.58
H9	5.69 ± 0.24	4.97 ± 0.28	6.88
Cter	7.42 ± 0.24	6.75 ± 0.08	3.01

from their pK_{mod} values, strongly favoring their neutral states. The pronounced positive shift observed for Cter is larger in the acylated isoform, while the negative shift of the H9 pK_a is larger in the deacylated form. Residues C5 and C6 rarely titrate, even at pH 8, and therefore, we can only predict their pK_a values to be higher than 8. In our previous work,[26] the observed titration shifts were attributed to persistent intraprotein interactions involving the titrating sites that occurred as a result of the lack of ability of the membrane-mimetic solution to stabilize the charged residues. However, such intraprotein interactions are not expected to play an important role in the lipid environment simulated here, as the titrating sites are expected to be located in the water/lipid interface or to interact with the surrounding lipid molecules. Therefore, the differences between the titrations of the two isoforms should rather be related to their distinct orientations in the bilayer and protein−lipid interactions, as discussed in sections 3.3 and 3.4.

3.3. Orientation of SP-C in the DPPC Bilayer. According to the available experimental data, the SP-C N-terminal region is expected to be near the lipid/water interface,[43,104,105] with some of the basic residues possibly buried in the membrane polar region.[43] When inserted into DPPC/DPPG bilayers at around pH 7, both SP-C isoforms have shown a predominantly parallel orientation of the long helix axis with respect to the lipid acyl chains, with an average angle of orientation of about 20° with respect to the bilayer normal for both isoforms.[96,97] More recently, Roldan et al.[51] also observed statistically similar tilt angles for both isoforms in multilayer membrane systems composed of three different lipid mixtures at different temperatures around pH 7.

To analyze the orientation of the protein in the pure DPPC bilayer simulated here, we followed the *z*-axis average positions of the N-terminal, H9, K11, R12, and C-terminal residues (Table 2 and Figure S14) and the tilt angles of the SP-C

Table 2. Time-Averaged Atomic Coordinates (in nm) of the N-Terminal Nitrogen Atom of the Amine Group (Nter), the Center of Mass of the H9 Imidazole Ring (H9), the Nitrogen Atom of the K11 Amine Group (K11), the Central Carbon Atom in the R12 Guanidinium Group (R12), and the Carbon Atom in the C-Terminal Carboxyl Group (Cter) Compared with the Average Positions of the Lipid Phosphorus Atoms (P) along the *z* Axis for the Equilibrated Segments of the (top) Acylated and (bottom) Deacylated SP-C Isoforms at Different pH Values[a]

	Acylated					
	pH 3	pH 4	pH 5	pH 6	pH 7	pH 8
P	−1.94	−1.94	−1.98	−1.95	−1.95	−1.97
Nter	−2.09	−2.07	−1.88	−2.14	−1.80	−2.21
H9	−1.93	−1.78	−1.84	−2.05	−2.12	−1.90
K11	−1.85	−2.09	−1.63	−2.11	−1.90	−1.88
R12	−1.65	−1.86	−1.68	−1.85	−1.73	−1.60
Cter	1.25	1.18	1.21	1.29	1.37	1.27
P	1.86	1.85	1.80	1.82	1.83	1.81
	Deacylated					
	pH 3	pH 4	pH 5	pH 6	pH 7	pH 8
P	−1.87	−1.92	−1.91	−1.91	−1.94	−1.91
Nter	−1.83	−1.95	−1.82	−1.97	−1.95	−2.06
H9	−1.14	−1.27	−1.34	−1.13	−1.15	−1.37
K11	−1.60	−1.65	−1.72	−1.48	−1.50	−1.66
R12	−1.34	−1.58	−1.68	−1.57	−1.49	−1.77
Cter	1.50	1.41	1.48	1.41	1.33	1.72
P	1.95	1.87	1.91	1.88	1.83	1.89

[a]The standard error of the averaged atomic coordinates was always lower than 0.08 nm.

transmembrane helix regions (residues 14−34 and 11−32 in the acylated and deacylated SP-C isoforms, respectively) relative to the bilayer normal (Figure 6) over the studied pH range. In agreement with the experimental observations, the Nter residue has an average location near the lipid/water interface, being mostly exposed to the aqueous environment in both isoforms. The average positions of H9, K11, and R12 coincide with the polar membrane region in two isoforms, but these residues are more buried in the deacylated case, especially H9. The Cter residue is always significantly buried in the membrane polar region in both isoforms, except at pH 8, where it has an average location closer to the lipid/water interfacial region in the deacylated isoform.

The results for the protein orientation in the DPPC bilayer can explain the pK_a values (Table 1) obtained from the titration curves depicted in Figure 5. While the Nter residue has a pK_a similar to its pK_{mod}, given its water exposure, the buried H9 and Cter residues exhibit considerable shifts from their pK_{mod} values. The fact that H9 in the deacylated isoform is more buried in comparison with the acylated case is consistent with the larger pK_{mod} shift obtained for this residue in the deacylated case. The degree of internalization of the Cter residue in the studied pH range explains the considerable pK_{mod} shifts

DOI: 10.1021/acs.jcim.5b00076
J. Chem. Inf. Model. 2015, 55, 2206−2217

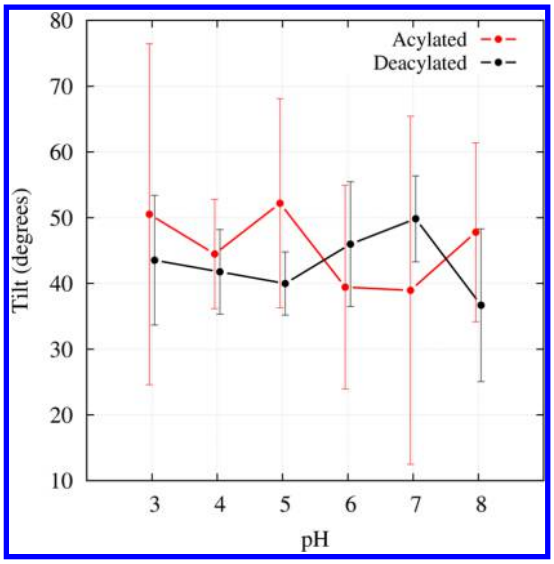

Figure 6. Tilt angles of the helix transmembrane region relative to the bilayer normal for the acylated (red line) and deacylated (black line) isoforms of SP-C at different pH values in the DPPC bilayer. For clarity of the error bars, the data for the acylated/deacylated forms are displaced by ∓0.04 pH units.

obtained for both isoforms, and the lower internalization in the deacylated isoform at pH 8 justifies the lower pK_{mod} shift obtained for the deacylated isoform. This relationship between the protein orientation in the membrane and the pK_a shifts of buried residues was previously observed experimentally for histidine-[106] and lysine-containing peptides.[85] The pK_a values obtained for H9 in the two isoforms were comparable with the experimental 4.9−6.6 range.[106]

There is no statistical diference between the tilt angles observed for the two isoforms, with average values ranging from 35 to 55°. Interestingly, the trend observed at pH 7 is comparable to the one observed by Roldan et al.[51] for the system with a lipid composition and temperature most similar to ours (DPPC/POPC films at 310.15 K), where the deacylated isoform exhibits an average tilt angle ∼10° higher than that of the acylated isoform. Overall, our computed values are higher than the ones observed experimentally,[51,96,97] which is also in agreement with the slight increase in the tilt angle for higher temperatures observed by Roldan et al.,[51] since we simulated the system at 323 K to keep the system above the DPPC phase transition temperature. Nevertheless, such differences can also arise from the use of different bilayer systems as well as the use of distinct methods to estimate the transmembrane helix tilt angles: while the experimental tilt angles were calculated from the measured polarized attenuated total reflectance (ATR) FTIR spectra of SP-C assuming an idealized helix model,[96,97,107] here we estimated the tilt angle as the angle between the first principal axis of the transmembrane helix region and the membrane normal. The relation between the two methods is nontrivial and dependent on model assumptions, and its clarification would require a back-calculation as done for the case of tilt angles inferred from solid-state NMR spectroscopy,[108] which was outside the scope of the present study. The tilt angles obtained in the present work are lower than the average tilt angles of 70 ± 5°[109] and 75−82°[101] obtained for the acylated and deacylated isoforms, respectively, in DPPC monolayers. This distinct orientation of SP-C molecules upon moving from bilayers to monolayers is thought to be important to maximize the protein−lipid contacts in these two different lipid contexts, illustrating the function of SP-C as a hydrophobic lever during the breathing cycle.

Comparing the results for the degree of internalization with the tilting behavior over the studied pH range, we observe some correlations for the two isoforms. In the acylated case, the adoption of less tilted conformations at pH 6 and 7 coincides with the H9, K11, and R12 residues being slightly less buried in the membrane. For the deacylated isoform, the larger tilt angle values obtained at pH 6 and 7 coincide with the H9, K11, and R12 residues being more buried in the membrane, and the less tilted conformations adopted at pH 8 can be related to the location of the (deprotonated) Cter residue near the lipid/water interface.

Altogether, the results in this section underline the correlation between the protein orientation preferences in a DPPC bilayer and its titration behavior, highlighting the relevance of the protonation−conformation coupling effects in the SP-C conformational behavior in a lipid environment.

3.4. Protein−Lipid Contacts. In our previous work,[26] we observed several persistent intraprotein contacts due to the inability of the molecules composing the membrane-mimetic mixture to properly stabilize charged residues of SP-C. However, these are not expected to be significant for the protein conformational behavior in a lipid environment, since the water molecules and the polar membrane region are likely to interact with the protein charges. Similar to what was done previously, the frequencies of intraprotein contacts involving the titratable residues were calculated, but no significant intraprotein contacts were observed in the acylated isoform. Contacts reaching a frequency of 25% were observed only in the deacylated form, namely between the H9 imidazole $N^{\delta 1}$ and N^{α} atoms at pH 7 and 8 and between the H9 imidazole $N^{\delta 1}$ and R12 guanidinium atoms at pH 6−8 (data not shown). These contacts may also contribute to the higher pK_{mod} shift obtained for the deacylated H9 residue (Figure 5 and Table 1). However, in contrast with the end-to-end interactions observed in our previous simulations,[26] such intraprotein interactions do not significantly affect the protein conformational behavior. Hence, we decided to focus our attention on the protein−lipid interactions.

ATR-FTIR measurements of SP-C inserted in DPPC monolayers showed that both isoforms interact with the lipid acyl chains,[101,109] but while the acylated isoform showed a preference for the *sn*-2 chain carbonyl group,[109] a similar semiquantitative analysis was not possible in the deacylated isoform experiments.[101] However, a preferential interaction with the carbonyl group of the *sn*-2 lipid chain is expected, given that its adjacent bend makes it more accessible than the *sn*-1 carbonyl group, as suggested by Gericke et al.[109] To investigate whether the charged residues of the protein have a preference for the lipid headgroup region or the acyl ester bonds, we analyzed the histograms of their distances to different lipid atoms over the studied pH range (Figures S15−S18).

For both isoforms, the basic sites (Nter, H9, K11, and R12) were observed to interact preferentially with the *sn*-2 carbonyl oxygen, in agreement with reported data.[109] However, in the deacylated isoform, some competing interactions involving H9 were more pronounced, namely, those with atoms in the phosphate group or the previously mentioned intraprotein interactions, which may be another contributing factor in making the pK_{mod} shift of this residue larger in this isoform. In

DOI: 10.1021/acs.jcim.5b00076
J. Chem. Inf. Model. 2015, 55, 2206−2217

general, the Cter carboxyl group preferentially adopts a position near the choline group and the acylated Cys thioester groups remain near the lipid headgroups, while the deacylated thiol groups interact with the charged phosphate oxygens. These persistent protein−lipid interactions accommodate the charged residues of the protein when they are buried in the membrane polar region, which is especially important to stabilize the basic N-terminal residues, whose local net charge can be as high as +4 depending on the pH simulated.

3.5. Membrane Properties. In this section, we investigate the effect of SP-C on the behavior of the surrounding lipids. We observed that the presence of the protein does not have a significant effect on the average area per lipid (Table 3 and Figure S19), the average bilayer thickness (Figure S20), the vertical position of the headgroups around it (Figure S21), or the dihedral angle distributions of the neighboring acyl chains (Figure S22). However, its presence promotes a significant increase in the area per lipid of neighboring lipid molecules (Table 3 and Figure S19), which is more pronounced in the N-terminal layer, especially in the presence of the acyl moieties. The ability to perturb the lipid packing was also observed experimentally in DPPC monolayers containing SP-C.[110,111]

Table 3. Time-Averaged Areas per Lipid (in nm^2) for the Acylated and Deacylated Isoforms of SP-C at Different pH Values in the DPPC Bilayer[a]

	Acylated			
	Nter layer		Cter layer	
pH	neighbor	all	neighbor	all
3	0.65	0.63	0.62	0.62
4	0.69	0.63	0.62	0.62
5	0.65	0.63	0.64	0.63
6	0.68	0.63	0.64	0.62
7	0.67	0.63	0.65	0.62
8	0.67	0.63	0.64	0.62
	Deacylated			
	Nter layer		Cter layer	
pH	neighbor	all	neighbor	all
3	0.63	0.63	0.65	0.62
4	0.66	0.63	0.64	0.63
5	0.65	0.63	0.63	0.62
6	0.67	0.63	0.64	0.63
7	0.66	0.64	0.65	0.63
8	0.68	0.63	0.64	0.63

[a]The area per lipid was measured separately for all of the lipids in the N-terminal and C-terminal layers (denoted as "all") and for all of the lipids within 5 Å of the protein in the N-terminal and C-terminal layers (denoted as "neighbor"). The standard error of the averaged atomic coordinates was always lower than 0.03 nm^2.

We also analyzed the lipid order parameters (Figure 7), and we observed that the presence of the acylated SP-C results in slightly higher values for the acyl chains of the neighboring lipid molecules in some cases, especially at lower pH. An ordering effect was reported by Gericke et al.,[109] but they were performing ATR-FTIR experiments using DPPC monolayers and focusing on the orientation of the lipid carbonyl groups.

3.6. Implications for the Physiological Role of SP-C in Lung Surfactant. Our results suggest that SP-C is highly stable in the membrane environment over the pH range simulated here, independent of the presence or absence of the acyl chains. The presence of the acyl moieties is here observed to contribute to a higher flexibility of the protein N-terminal end while keeping the transmembrane region rigid. This might be related to the proposed physiological role of the acylated SP-C isoform in stabilizing the surfactant reservoirs:[1−3] while some flexibility in the N-terminal region would be required for attachment of the protein to adjacent bilayers, a low plasticity in the transmembrane domain would stabilize these multilayered membrane structures.

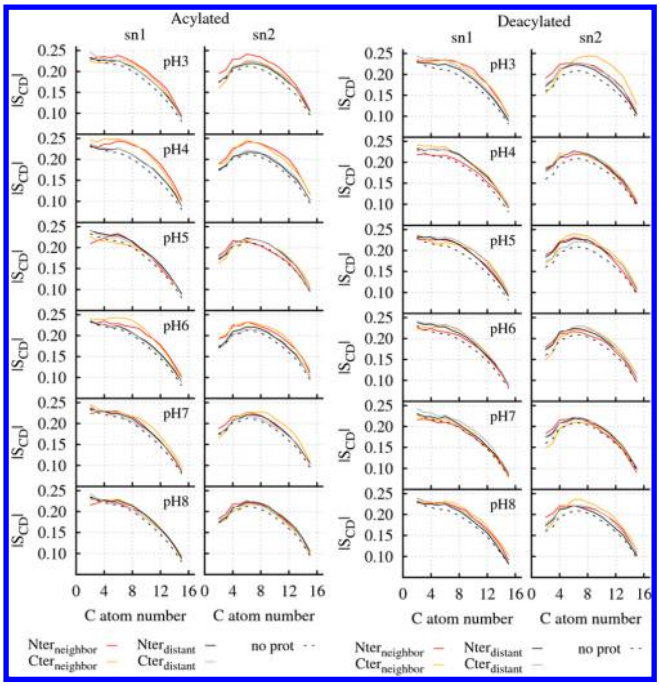

Figure 7. Lipid order parameters for the neighboring lipid molecules (within a spherical cutoff of 0.5 nm around the protein) in the N-terminal (red solid lines) and C-terminal (orange solid lines) layers and for the distant lipid molecules (outside a spherical cutoff of 0.5 nm around the protein) in the N-terminal (black solid lines) and C-terminal (gray solid lines) layers. The lipid *sn*-1 and *sn*-2 acyl chains were analyzed separately. The results are presented for the (left) acylated and (right) deacylated SP-C isoforms at different pH values and are compared with the order parameters obtained for the equilibrated pure DPPC bilayers (dashed lines).

The titratable residues of SP-C have often been suggested to play a role in its mechanism of action.[42−48] We observe that these residues maintain persistent interactions with specific polar groups of the surrounding DPPC molecules that mediate their degrees of membrane internalization (which are sometimes different in the acylated and deacylated isoforms) and the protein tilting behavior. Some local interaction preferences show some dependence on the pH, but this does not seem to have an overall effect on the protein stability and/or the dynamic behavior of the neighboring lipids. This is in line with experimental evidence that the surface properties of the pulmonary surfactant appear to be relatively insensitive to the alveolar subphase pH,[112] at least concerning the contribution of SP-C to the surfactant film stability.

Although they are assumed to be zwitterionic over the pH range simulated here, a minor population of the phosphate group in PC lipids is likely to be protonated at pH $\leq$ 4,[113,114] making the overall charge of some lipid molecules positive. This could possibly lead to local repulsive interactions among non-zwitterionic DPPC molecules and/or between these and the

DOI: 10.1021/acs.jcim.5b00076
J. Chem. Inf. Model. 2015, 55, 2206−2217

basic residues in the SP-C N-terminal region, which might affect both the protein stability and the lipids' dynamic behavior. Such an effect could be taken into account by treating the lipids as titrating molecules,[75] but this would be computationally more expensive and possibly make a negligible contribution to the system dynamics. Also, a drop in the pH of the alveolar subphase to values lower than 5 (or a rise to values higher than 7) is unlikely. Therefore, our simulations under such extreme pH conditions are intended not to depict a realistic physiological/pathological scenario but rather to allow comparison to former studies.[25,26]

Finally, SP-C is observed to affect the conformational behavior of lipid molecules in its vicinity by significantly disturbing the lateral lipid packing. This may result from the persistent protein−lipid interactions observed in this study and may mediate the functional action of SP-C in the lung surfactant.[2,3,7,11−15] It should be noted that the presence of negatively charged lipids (e.g., phosphatidylglycerol, which constitutes up to approximately 10% of the pulmonary surfactant) may influence the measured membrane properties, as they would be expected to establish stronger electrostatic interactions with the SP-C N-terminal basic residues.

4. CONCLUSION

In this work, the conformational behavior of both the acylated and deacylated SP-C isoforms has been studied in a pure DPPC bilayer under different pH conditions using constant-pH MD simulations, accounting for a total of 3 μs of simulation time for each isoform. Our results highlight the remarkable stability of both SP-C isoforms while inserted in a DPPC bilayer and the structural effects of deacylation on the protein conformational behavior over the studied pH range. Although it has a similar helical content, the acylated isoform exhibits a shortened transmembrane helix segment, adopting a labile helix−turn−helix motif in the N-terminal region, which is rarely observed in the simulations of the deacylated isoform. We have estimated similar tilt angles for the two isoforms over the studied pH range, with a generally higher degree of internalization of the basic N-terminal residues in the deacylated case, and have observed and discussed some protonation−conformation coupling effects. Similar preferences to interact with different lipid atoms are exhibited by the two isoforms, with the Nter, H9, K11, and R12 contacting more frequently with the carbonyl oxygen atoms in the *sn*-2 acyl chains and the C5, C6, and Cter residues with the lipid headgroup region. Also, the presence of SP-C significantly alters the local lateral packing of the membrane. No pH trend was observed, although the pH affects the protein conformational behavior and the establishment of protein−lipid contacts in some cases.

The similar helical contents and tilt angles for the two isoforms agree with recent experimental observations.[51] Furthermore, the contrasting results for SP-C behavior in a lipid environment and in a membrane-mimetic solution[26] clearly show that a membrane environment is essential for understanding the effects taking part in the SP-C structure stabilization and the specific functions of SP-C in the lung surfactant film. However, to fully understand the molecular mechanism through which the protein fulfills its function, its interfacial behavior while it is inserted in a monolayer system and submitted to different surface tension conditions and the use of more complex lipid systems are some of the features that need to be considered in the future.

■ ASSOCIATED CONTENT

Supporting Information

The Supporting Information is available free of charge on the ACS Publications website at DOI: 10.1021/acs.jcim.5b00076.

Cartoon representation of SP-C, percentages of total helix structure, percentages of helix per residue, Hill coefficients per titrable site, cumulative protonation averages per titrable site, individual Hill curves per titrable site, time-averaged degrees of internalization per titrable site, identified protein−lipid interactions, areas per lipid, membrane thicknesses, average *z*-axis positions of the lipid phosphorus atoms according to their distances to the protein, and acyl chain dihedral angle distributions (PDF)

■ AUTHOR INFORMATION

Corresponding Authors

*E-mail: baptista@itqb.unl.pt.
*E-mail: scampos@itqb.unl.pt.

Present Address

†C.A.C.: School of Life Sciences, University of Dundee, Dundee DD1 5EH, U.K.

Notes

The authors declare no competing financial interest.

■ ACKNOWLEDGMENTS

This study was supported by Fundação para a Ciência e Tecnologia through Grants PTDC/QUI-BIQ/105238/2008, PTDC/BIA-PRO/104378/2008, PTDC/QEQ-COM/1623/2012, and PEst-OE/EQB/LA0004/2011.

■ ABBREVIATIONS

SP-C, surfactant protein C; DPPC, dipalmitoylphosphatidylcholine; MD, molecular dynamics; PDB, Protein Data Bank; MM, molecular mechanics; PB, Poisson−Boltzmann; MC, Monte Carlo; rmsf, root-mean-square fluctuation

■ REFERENCES

(1) Zuo, Y. Y.; Veldhuizen, R. A. W.; Neumann, A. W.; Petersen, N. O.; Possmayer, F. Current Perspectives in Pulmonary Surfactant–Inhibition, Enhancement and Evaluation. *Biochim. Biophys. Acta, Biomembr.* **2008**, *1778*, 1947−1977.

(2) Perez-Gil, J.; Weaver, T. E. Pulmonary Surfactant Pathophysiology: Current Models and Open Questions. *Physiology* **2010**, *25*, 132−141.

(3) Zuo, Y. Y.; Keating, E.; Zhao, L.; Tadayyon, S. M.; Veldhuizen, R. A. W.; Petersen, N. O.; Possmayer, F. Atomic Force Microscopy Studies of Functional and Dysfunctional Pulmonary Surfactant Films. I. Micro- and Nanostructures of Functional Pulmonary Surfactant Films and the Effect of SP-A. *Biophys. J.* **2008**, *94*, 3549−3564.

(4) Galla, H.-J.; Bourdos, N.; von Nahmen, A.; Amrein, M.; Sieber, M. The Role of Pulmonary Surfactant Protein C during the Breathing Cycle. *Thin Solid Films* **1998**, *327−329*, 632−635.

(5) Weaver, T. E. Synthesis, Processing and Secretion of Surfactant Proteins B and C. *Biochim. Biophys. Acta, Mol. Basis Dis.* **1998**, *1408*, 173−179.

(6) Haagsman, H. P.; Diemel, R. V. Surfactant-Associated Proteins: Functions and Structural Variation. *Comp. Biochem. Physiol., Part A: Mol. Integr. Physiol.* **2001**, *129*, 91−108.

(7) Ten Brinke, A.; van Golde, L. M. G.; Batenburg, J. J. Palmitoylation and Processing of the Lipopeptide Surfactant Protein C. *Biochim. Biophys. Acta, Mol. Cell Biol. Lipids* **2002**, *1583*, 253−265.

DOI: 10.1021/acs.jcim.5b00076
J. Chem. Inf. Model. 2015, 55, 2206−2217

(8) Johansson, J.; Persson, P.; Löwenadler, B.; Robertson, B.; Jörnvall, H.; Curstedt, T. Canine Hydrophobic Surfactant Polypeptide SP-C A Lipopeptide with One Thioester-Linked Palmitoyl Group. *FEBS Lett.* **1991**, *281*, 119−122.
(9) Johansson, J.; Szyperski, T.; Curstedt, T.; Wüthrich, K. The NMR Structure of the Pulmonary Surfactant-Associated Polypeptide SP-C in an Apolar Solvent Contains a Valyl-Rich Alpha-Helix. *Biochemistry* **1994**, *33*, 6015−6023.
(10) Johansson, J. Structure and Properties of Surfactant Protein C. *Biochim. Biophys. Acta, Mol. Basis Dis.* **1998**, *1408*, 161−172.
(11) Taneva, S.; Keough, K. M. Pulmonary Surfactant Proteins SP-B and SP-C in Spread Monolayers at the Air-Water Interface: II. Monolayers of Pulmonary Surfactant Protein SP-C and Phospholipids. *Biophys. J.* **1994**, *66*, 1149−1157.
(12) Takamoto, D. Y.; Lipp, M. M.; von Nahmen, A.; Lee, K. Y.; Waring, A. J.; Zasadzinski, J. A. Interaction of Lung Surfactant Proteins with Anionic Phospholipids. *Biophys. J.* **2001**, *81*, 153−169.
(13) Wang, L.; Cai, P.; Galla, H.-J.; He, H.; Flach, C. R.; Mendelsohn, R. Monolayer-Multilayer Transitions in a Lung Surfactant Model: IR Reflection-Absorption Spectroscopy and Atomic Force Microscopy. *Eur. Biophys. J.* **2005**, *34*, 243−254.
(14) Pérez-Gil, J. Structure of Pulmonary Surfactant Membranes and Films: The Role of Proteins and Lipid−protein Interactions. *Biochim. Biophys. Acta, Biomembr.* **2008**, *1778*, 1676−1695.
(15) Mulugeta, S.; Beers, M. F. Surfactant Protein C: Its Unique Properties and Emerging Immunomodulatory Role in the Lung. *Microbes Infect.* **2006**, *8*, 2317−2323.
(16) Lukovic, D.; Cruz, A.; Gonzalez-Horta, A.; Almlen, A.; Curstedt, T.; Mingarro, I.; Pérez-Gil, J. Interfacial Behavior of Recombinant Forms of Human Pulmonary Surfactant Protein SP-C. *Langmuir* **2012**, *28*, 7811−7825.
(17) Whitsett, J. A.; Wert, S. E.; Weaver, T. E. Alveolar Surfactant Homeostasis and the Pathogenesis of Pulmonary Disease. *Annu. Rev. Med.* **2010**, *61*, 105−119.
(18) Gustafsson, M.; Thyberg, J.; Näslund, J.; Eliasson, E.; Johansson, J. Amyloid Fibril Formation by Pulmonary Surfactant Protein C. *FEBS Lett.* **1999**, *464*, 138−142.
(19) Seymour, J. F.; Presneill, J. J. Pulmonary Alveolar Proteinosis: Progress in the First 44 Years. *Am. J. Respir. Crit. Care Med.* **2002**, *166*, 215−235.
(20) Presneill, J. J.; Nakata, K.; Inoue, Y.; Seymour, J. F. Pulmonary Alveolar Proteinosis. *Clin. Chest Med.* **2004**, *25*, 593−613.
(21) Kallberg, Y.; Gustafsson, M.; Persson, B.; Thyberg, J.; Johansson, J. Prediction of Amyloid Fibril-Forming Proteins. *J. Biol. Chem.* **2001**, *276*, 12945−12950.
(22) Johansson, J.; Nilsson, G.; Strömberg, R.; Robertson, B.; Jörnvall, H.; Curstedt, T. Secondary Structure and Biophysical Activity of Synthetic Analogues of the Pulmonary Surfactant Polypeptide SP-C. *Biochem. J.* **1995**, *307*, 535−541.
(23) Wang, Z.; Gurel, O.; Baatz, J. E.; Notter, R. H. Acylation of Pulmonary Surfactant Protein-C Is Required for Its Optimal Surface Active Interactions with Phospholipids. *J. Biol. Chem.* **1996**, *271*, 19104−19109.
(24) Yousefi-Salakdeh, E.; Johansson, J.; Strömberg, R. A Method for S- and O-Palmitoylation of Peptides: Synthesis of Pulmonary Surfactant Protein-C Models. *Biochem. J.* **1999**, *343*, 557−562.
(25) Dluhy, R. A.; Shanmukh, S.; Leapard, J. B.; Krüger, P.; Baatz, J. E. Deacylated Pulmonary Surfactant Protein SP-C Transforms from Alpha-Helical to Amyloid Fibril Structure via a pH-Dependent Mechanism: An Infrared Structural Investigation. *Biophys. J.* **2003**, *85*, 2417−2429.
(26) Carvalheda, C. A.; Campos, S. R. R.; Machuqueiro, M.; Baptista, A. M. Structural Effects of pH and Deacylation on Surfactant Protein C in an Organic Solvent Mixture: A Constant-pH MD Study. *J. Chem. Inf. Model.* **2013**, *53*, 2979−2989.
(27) Omary, M. B.; Trowbridge, I. S. Biosynthesis of the Human Transferrin Receptor in Cultured Cells. *J. Biol. Chem.* **1981**, *256*, 12888−12892.
(28) Basu, J. Protein Palmitoylation and Dynamic Modulation of Protein Function. *Curr. Sci.* **2004**, *87*, 212−217.
(29) Ng, A. W.; Bidani, A.; Heming, T. A. Innate Host Defense of the Lung: Effects of Lung-Lining Fluid pH. *Lung* **2004**, *182*, 297−317.
(30) Johansson, J.; Weaver, T. E.; Tjernberg, L. O. Proteolytic Generation and Aggregation of Peptides from Transmembrane Regions: Lung Surfactant Protein C and Amyloid Beta-Peptide. *Cell. Mol. Life Sci.* **2004**, *61*, 326−335.
(31) Baoukina, S.; Monticelli, L.; Amrein, M.; Tieleman, D. P. The Molecular Mechanism of Monolayer-Bilayer Transformations of Lung Surfactant from Molecular Dynamics Simulations. *Biophys. J.* **2007**, *93*, 3775−3782.
(32) Baoukina, S.; Tieleman, D. P. Direct Simulation of Protein-Mediated Vesicle Fusion: Lung Surfactant Protein B. *Biophys. J.* **2010**, *99*, 2134−2142.
(33) Duncan, S. L.; Larson, R. G. Folding of Lipid Monolayers Containing Lung Surfactant Proteins SP-B(1−25) and SP-C Studied via Coarse-Grained Molecular Dynamics Simulations. *Biochim. Biophys. Acta, Biomembr.* **2010**, *1798*, 1632−1650.
(34) Kovacs, H.; Mark, A. E.; Johansson, J.; van Gunsteren, W. F. The Effect of Environment on the Stability of an Integral Membrane Helix: Molecular Dynamics Simulations of Surfactant Protein C in Chloroform, Methanol and Water. *J. Mol. Biol.* **1995**, *247*, 808−822.
(35) Kovacs, H.; Mark, A. E.; van Gunsteren, W. F. Solvent Structure at a Hydrophobic Protein Surface. *Proteins: Struct., Funct., Genet.* **1997**, *27*, 395−404.
(36) Ramírez, E.; Santana, A.; Cruz, A.; Plasencia, I.; López, G. E. Molecular Dynamics of Surfactant Protein C: From Single Molecule to Heptameric Aggregates. *Biophys. J.* **2006**, *90*, 2698−2705.
(37) Baptista, A. M.; Teixeira, V. H.; Soares, C. M. Constant-pH Molecular Dynamics Using Stochastic Titration. *J. Chem. Phys.* **2002**, *117*, 4184−4200.
(38) Machuqueiro, M.; Baptista, A. M. Constant-pH Molecular Dynamics with Ionic Strength Effects: Protonation−Conformation Coupling in Decalysine. *J. Phys. Chem. B* **2006**, *110*, 2927−2933.
(39) Machuqueiro, M.; Baptista, A. M. Acidic Range Titration of HEWL Using a Constant-pH Molecular Dynamics Method. *Proteins: Struct., Funct., Genet.* **2008**, *72*, 289−298.
(40) Machuqueiro, M.; Baptista, A. M. Is the Prediction of pKa Values by Constant-pH Molecular Dynamics Being Hindered by Inherited Problems? *Proteins: Struct., Funct., Genet.* **2011**, *79*, 3437−3447.
(41) Magalhães, P. R.; Machuqueiro, M.; Baptista, A. M. Constant-pH Molecular Dynamics Study of Kyotorphin in an Explicit Bilayer. *Biophys. J.* **2015**, *108*, 2282−2290.
(42) Creuwels, L. A.; Demel, R. A.; van Golde, L. M.; Benson, B. J.; Haagsman, H. P. Effect of Acylation on Structure and Function of Surfactant Protein C at the Air-Liquid Interface. *J. Biol. Chem.* **1993**, *268*, 26752−26758.
(43) Morrow, M. R.; Taneva, S.; Simatos, G. A.; Allwood, L. A.; Keough, K. M. 2H NMR Studies of the Effect of Pulmonary Surfactant SP-C on the 1,2-Dipalmitoyl-Sn-Glycero-3-Phosphocholine Headgroup: A Model for Transbilayer Peptides in Surfactant and Biological Membranes. *Biochemistry* **1993**, *32*, 11338−11344.
(44) Creuwels, L. A.; Demel, R. A.; van Golde, L. M.; Haagsman, H. P. Characterization of a Dimeric Canine Form of Surfactant Protein C (SP-C). *Biochim. Biophys. Acta, Lipids Lipid Metab.* **1995**, *1254*, 326−332.
(45) Pérez-Gil, J.; Casals, C.; Marsh, D. Interactions of Hydrophobic Lung Surfactant Proteins SP-B and SP-C with Dipalmitoylphosphatidylcholine and Dipalmitoylphosphatidylglycerol Bilayers Studied by Electron Spin Resonance Spectroscopy. *Biochemistry* **1995**, *34*, 3964−3971.
(46) Krüger, P.; Schalke, M.; Wang, Z.; Notter, R. H.; Dluhy, R. A.; Lösche, M. Effect of Hydrophobic Surfactant Peptides SP-B and SP-C on Binary Phospholipid Monolayers. I. Fluorescence and Dark-Field Microscopy. *Biophys. J.* **1999**, *77*, 903−914.

DOI: 10.1021/acs.jcim.5b00076
J. Chem. Inf. Model. 2015, 55, 2206−2217

(47) Plasencia, I.; Cruz, A.; López-Lacomba, J. L.; Casals, C.; Pérez-Gil, J. Selective Labeling of Pulmonary Surfactant Protein SP-C in Organic Solution. *Anal. Biochem.* **2001**, *296*, 49−56.
(48) Bi, X.; Flach, C. R.; Pérez-Gil, J.; Plasencia, I.; Andreu, D.; Oliveira, E.; Mendelsohn, R. Secondary Structure and Lipid Interactions of the N-Terminal Segment of Pulmonary Surfactant SP-C in Langmuir Films: IR Reflection-Absorption Spectroscopy and Surface Pressure Studies. *Biochemistry* **2002**, *41*, 8385−8395.
(49) Qanbar, R.; Possmayer, F. On the Surface Activity of Surfactant-Associated Protein C (SP-C): Effects of Palmitoylation and pH. *Biochim. Biophys. Acta, Lipids Lipid Metab.* **1995**, *1255*, 251−259.
(50) Camacho, L.; Cruz, A.; Castro, R.; Casals, C.; Pérez-Gil, J. Effect of pH on the Interfacial Adsorption Activity of Pulmonary Surfactant. *Colloids Surf., B* **1996**, *5*, 271−277.
(51) Roldan, N.; Goormaghtigh, E.; Pérez-Gil, J.; Garcia-Alvarez, B. Palmitoylation as a Key Factor to Modulate SP-C-Lipid Interactions in Lung Surfactant Membrane Multilayers. *Biochim. Biophys. Acta, Biomembr.* **2015**, *1848*, 184−191.
(52) DeLano, W. L. The PyMOL Molecular Graphics System. www.pymol.org (accessed Sept 19, 2012).
(53) Schuler, L. D.; Daura, X.; van Gunsteren, W. F. An Improved GROMOS96 Force Field for Aliphatic Hydrocarbons in the Condensed Phase. *J. Comput. Chem.* **2001**, *22*, 1205−1218.
(54) Berendsen, H. J. C.; van der Spoel, D.; van Drunen, R. GROMACS: A Message-Passing Parallel Molecular Dynamics Implementation. *Comput. Phys. Commun.* **1995**, *91*, 43−56.
(55) Hess, B.; Kutzner, C.; van der Spoel, D.; Lindahl, E. GROMACS 4: Algorithms for Highly Efficient, Load-Balanced, and Scalable Molecular Simulation. *J. Chem. Theory Comput.* **2008**, *4*, 435−447.
(56) Mabrey, S.; Sturtevant, J. M. Investigation of Phase Transitions of Lipids and Lipid Mixtures by Sensitivity Differential Scanning Calorimetry. *Proc. Natl. Acad. Sci. U. S. A.* **1976**, *73*, 3862−3866.
(57) Huang, C. H.; Lapides, J. R.; Levin, I. W. Phase-Transition Behavior of Saturated, Symmetric Chain Phospholipid Bilayer Dispersions Determined by Raman Spectroscopy: Correlation between Spectral and Thermodynamic Parameters. *J. Am. Chem. Soc.* **1982**, *104*, 5926−5930.
(58) Bussi, G.; Donadio, D.; Parrinello, M. Canonical Sampling through Velocity Rescaling. *J. Chem. Phys.* **2007**, *126*, 014101.
(59) Berendsen, H. J. C.; Postma, J. P. M.; van Gunsteren, W. F.; DiNola, A.; Haak, J. R. Molecular Dynamics with Coupling to an External Bath. *J. Chem. Phys.* **1984**, *81*, 3684−3690.
(60) Poger, D.; Van Gunsteren, W. F.; Mark, A. E. A New Force Field for Simulating Phosphatidylcholine Bilayers. *J. Comput. Chem.* **2010**, *31*, 1117−1125.
(61) Poger, D.; Mark, A. E. On the Validation of Molecular Dynamics Simulations of Saturated and Cis-Monounsaturated Phosphatidylcholine Lipid Bilayers: A Comparison with Experiment. *J. Chem. Theory Comput.* **2010**, *6*, 325−336.
(62) Barker, J. A.; Watts, R. O. Monte Carlo Studies of the Dielectric Properties of Water-like Models. *Mol. Phys.* **1973**, *26*, 789−792.
(63) Tironi, I. G.; Sperb, R.; Smith, P. E.; van Gunsteren, W. F. A Generalized Reaction Field Method for Molecular Dynamics Simulations. *J. Chem. Phys.* **1995**, *102*, 5451.
(64) Hess, B.; Bekker, H.; Berendsen, H. J. C.; Fraaije, J. G. E. M. LINCS: A Linear Constraint Solver for Molecular Simulations. *J. Comput. Chem.* **1997**, *18*, 1463−1472.
(65) Schmid, N.; Eichenberger, A. P.; Choutko, A.; Riniker, S.; Winger, M.; Mark, A. E.; van Gunsteren, W. F. Definition and Testing of the GROMOS Force-Field Versions 54A7 and 54B7. *Eur. Biophys. J.* **2011**, *40*, 843−856.
(66) Domański, J.; Stansfeld, P. J.; Sansom, M. S. P.; Beckstein, O. Lipidbook: A Public Repository for Force-Field Parameters Used in Membrane Simulations. *J. Membr. Biol.* **2010**, *236*, 255−258.
(67) Hermans, J.; Berendsen, H. J. C.; Van Gunsteren, W. F.; Postma, J. P. M. A Consistent Empirical Potential for Water−protein Interactions. *Biopolymers* **1984**, *23*, 1513−1518.
(68) Press, W. H.; Teukolsky, S. A.; Vetterling, W. T.; Flannery, B. P. *Numerical Recipes in C++: The Art of Scientific Computing*, 2nd ed.; Cambridge University Press: Cambridge, U.K., 2002.
(69) Schmidt, T. H.; Kandt, C. LAMBADA and InflateGRO2: Efficient Membrane Alignment and Insertion of Membrane Proteins for Molecular Dynamics Simulations. *J. Chem. Inf. Model.* **2012**, *52*, 2657−2669.
(70) Campos, S. R. R.; Machuqueiro, M.; Baptista, A. M. Constant-pH Molecular Dynamics Simulations Reveal a B-Rich Form of the Human Prion Protein. *J. Phys. Chem. B* **2010**, *114*, 12692−12700.
(71) Vila-Viçosa, D.; Campos, S. R. R.; Baptista, A. M.; Machuqueiro, M. Reversibility of Prion Misfolding: Insights from Constant-pH Molecular Dynamics Simulations. *J. Phys. Chem. B* **2012**, *116*, 8812−8821.
(72) Vila-Viçosa, D.; Teixeira, V. H.; Santos, H. A. F.; Machuqueiro, M. Conformational Study of GSH and GSSG Using Constant-pH Molecular Dynamics Simulations. *J. Phys. Chem. B* **2013**, *117*, 7507−7517.
(73) Machuqueiro, M.; Baptista, A. M. Molecular Dynamics at Constant pH and Reduction Potential: Application to Cytochrome c(3). *J. Am. Chem. Soc.* **2009**, *131*, 12586−12594.
(74) Machuqueiro, M.; Baptista, A. M. The pH-Dependent Conformational States of Kyotorphin: A Constant-pH Molecular Dynamics Study. *Biophys. J.* **2007**, *92*, 1836−1845.
(75) Vila-Viçosa, D.; Teixeira, V. H.; Baptista, A. M.; Machuqueiro, M. Constant-pH MD Simulations of an Oleic Acid Bilayer. *J. Chem. Theory Comput.* **2015**, *11*, 2367−2376.
(76) Bashford, D.; Gerwert, K. Electrostatic Calculations of the pKa Values of Ionizable Groups in Bacteriorhodopsin. *J. Mol. Biol.* **1992**, *224*, 473−486.
(77) Teixeira, V. H.; Cunha, C. A.; Machuqueiro, M.; Oliveira, A. S. F.; Victor, B. L.; Soares, C. M.; Baptista, A. M. On the Use of Different Dielectric Constants for Computing Individual and Pairwise Terms in Poisson-Boltzmann Studies of Protein Ionization Equilibrium. *J. Phys. Chem. B* **2005**, *109*, 14691−14706.
(78) Machuqueiro, M.; Campos, S. R. R.; Soares, C. M.; Baptista, A. M. Membrane-Induced Conformational Changes of Kyotorphin Revealed by Molecular Dynamics Simulations. *J. Phys. Chem. B* **2010**, *114*, 11659−11667.
(79) Henriques, J.; Costa, P. J.; Calhorda, M. J.; Machuqueiro, M. Charge Parametrization of the DvH-c3 Heme Group: Validation Using Constant-(pH,E) Molecular Dynamics Simulations. *J. Phys. Chem. B* **2013**, *117*, 70−82.
(80) Baker, N. A.; Bashford, D.; Case, D. A. In *Implicit Solvent Electrostatics in Biomolecular Simulation*; Lecture Notes in Computational Science and Engineering, Vol. *49*; Springer: Berlin, 2006; Part V, pp 263−295.
(81) Carvalheda, C. A.; Campos, S. R. R.; Machuqueiro, M.; Baptista, A. M. Correction to "Structural Effects of pH and Deacylation on Surfactant Protein C in an Organic Solvent Mixture: A Constant-pH MD Study. *J. Chem. Inf. Model.* **2015**, *55*, 206−206.
(82) Baptista, A.; Soares, C. Some Theoretical and Computational Aspects of the Inclusion of Proton Isomerism in the Protonation Equilibrium of Proteins. *J. Phys. Chem. B* **2001**, *105*, 293−309.
(83) Baptista, A. M.; Martel, P. J.; Soares, C. M. Simulation of Electron-Proton Coupling with a Monte Carlo Method: Application to Cytochrome c3 Using Continuum Electrostatics. *Biophys. J.* **1999**, *76*, 2978−2998.
(84) Metropolis, N.; Rosenbluth, A.; Rosenbluth, M.; Teller, A.; Teller, E. Equation of State Calculations by Fast Computing Machines. *J. Chem. Phys.* **1953**, *21*, 1087−1092.
(85) Gleason, N. J.; Vostrikov, V. V.; Greathouse, D. V.; Koeppe, R. E. Buried Lysine, but Not Arginine, Titrates and Alters Transmembrane Helix Tilt. *Proc. Natl. Acad. Sci. U. S. A.* **2013**, *110*, 1692−1695.
(86) Panahi, A.; Brooks, C. L. Membrane Environment Modulates the pKa Values of Transmembrane Helices. *J. Phys. Chem. B* **2015**, *119*, 4601−4607.

DOI: 10.1021/acs.jcim.5b00076
J. Chem. Inf. Model. 2015, 55, 2206−2217

(87) Fitch, C. A.; Platzer, G.; Okon, M.; Garcia-Moreno E., B.; McIntosh, L. P. Arginine: Its pKa Value Revisited. *Protein Sci.* **2015**, *24*, 752−761.
(88) Lukat, G.; Krüger, J.; Sommer, B. APL@Voro: A Voronoi-Based Membrane Analysis Tool for GROMACS Trajectories. *J. Chem. Inf. Model.* **2013**, *53*, 2908−2925.
(89) Kabsch, W.; Sander, C. Dictionary of Protein Secondary Structure: Pattern Recognition of Hydrogen-Bonded and Geometrical Features. *Biopolymers* **1983**, *22*, 2577−2637.
(90) Campos, S. R. R.; Baptista, A. M. Confomational Analysis in a Multidimensional Energy Landscape: Study of an Arginylglutamate Repeat. *J. Phys. Chem. B* **2009**, *113*, 15989−16001.
(91) Goldstein, H. *Classical Mechanics*, 2nd ed.; Addison-Wesley: Reading, MA, 1980.
(92) Allen, M. P.; Tildesley, D. J. *Computer Simulation of Liquids*; Clarendon Press: Oxford, U.K., 1987.
(93) Bertsekas, D. P.; Tsitsiklis, J. N. *Introduction to Probability*; Athena Scientific: Belmont, MA, 2002.
(94) Gnuplot. http://www.gnuplot.info/ (accessed Sept 20, 2012).
(95) Efron, B.; Tibshirani, R. J. *An Introduction to the Bootstrap*; Chapman and Hall/CRC Press: Boca Raton, FL, 1993.
(96) Pastrana, B.; Mautone, A. J.; Mendelsohn, R. Fourier Transform Infrared Studies of Secondary Structure and Orientation of Pulmonary Surfactant SP-C and Its Effect on the Dynamic Surface Properties of Phospholipids. *Biochemistry* **1991**, *30*, 10058−10064.
(97) Vandenbussche, G.; Clercx, A.; Curstedt, T.; Johansson, J.; Jörnvall, H.; Ruysschaert, J. M. Structure and Orientation of the Surfactant-Associated Protein C in a Lipid Bilayer. *Eur. J. Biochem.* **1992**, *203*, 201−209.
(98) Horowitz, A. D.; Baatz, J. E.; Whitsett, J. A. Lipid Effects on Aggregation of Pulmonary Surfactant Protein SP-C Studied by Fluorescence Energy Transfer. *Biochemistry* **1993**, *32*, 9513−9523.
(99) Pérez-Gil, J.; Cruz, A.; Casals, C. Solubility of Hydrophobic Surfactant Proteins in Organic Solvent/water Mixtures. Structural Studies on SP-B and SP-C in Aqueous Organic Solvents and Lipids. *Biochim. Biophys. Acta, Lipids Lipid Metab.* **1993**, *1168*, 261−270.
(100) Shiffer, K.; Hawgood, S.; Haagsman, H. P.; Benson, B.; Clements, J. A.; Goerke, J. Lung Surfactant Proteins, SP-B and SP-C, Alter the Thermodynamic Properties of Phospholipid Membranes: A Differential Calorimetry Study. *Biochemistry* **1993**, *32*, 590−597.
(101) Flach, C. R.; Gericke, A.; Keough, K. M.; Mendelsohn, R. Palmitoylation of Lung Surfactant Protein SP-C Alters Surface Thermodynamics, but Not Protein Secondary Structure or Orientation in 1,2-Dipalmitoylphosphatidylcholine Langmuir Films. *Biochim. Biophys. Acta, Biomembr.* **1999**, *1416*, 11−20.
(102) Johansson, J.; Curstedt, T. Molecular Structures and Interactions of Pulmonary Surfactant Components. *Eur. J. Biochem.* **1997**, *244*, 675−693.
(103) Plasencia, I.; Rivas, L.; Casals, C.; Keough, K. M.; Pérez-Gil, J. Intrinsic Structural Differences in the N-Terminal Segment of Pulmonary Surfactant Protein SP-C from Different Species. *Comp. Biochem. Physiol., Part A: Mol. Integr. Physiol.* **2001**, *129*, 129−139.
(104) Plasencia, I.; Cruz, A.; Casals, C.; Pérez-Gil, J. Superficial Disposition of the N-Terminal Region of the Surfactant Protein SP-C and the Absence of Specific SP-B-SP-C Interactions in Phospholipid Bilayers. *Biochem. J.* **2001**, *359*, 651−659.
(105) Plasencia, I.; Rivas, L.; Keough, K. M. W.; Marsh, D.; Pérez-Gil, J. The N-Terminal Segment of Pulmonary Surfactant Lipopeptide SP-C Has Intrinsic Propensity to Interact with and Perturb Phospholipid Bilayers. *Biochem. J.* **2004**, *377*, 183−193.
(106) Bechinger, B. Towards Membrane Protein Design: pH-Sensitive Topology of Histidine-Containing Polypeptides. *J. Mol. Biol.* **1996**, *263*, 768−775.
(107) Brauner, J. W.; Mendelsohn, R.; Prendergast, F. G. Attenuated Total Reflectance Fourier Transform Infrared Studies of the Interaction of Melittin, Two Fragments of Melittin, and Delta-Hemolysin with Phosphatidylcholines. *Biochemistry* **1987**, *26*, 8151−8158.
(108) Ozdirekcan, S.; Etchebest, C.; Killian, J. A.; Fuchs, P. F. J. On the Orientation of a Designed Transmembrane Peptide: Toward the Right Tilt Angle? *J. Am. Chem. Soc.* **2007**, *129*, 15174−15181.
(109) Gericke, A.; Flach, C. R.; Mendelsohn, R. Structure and Orientation of Lung Surfactant SP-C and L-Alpha-Dipalmitoylphosphatidylcholine in Aqueous Monolayers. *Biophys. J.* **1997**, *73*, 492−499.
(110) Pérez-Gil, J.; Nag, K.; Taneva, S.; Keough, K. M. Pulmonary Surfactant Protein SP-C Causes Packing Rearrangements of Dipalmitoylphosphatidylcholine in Spread Monolayers. *Biophys. J.* **1992**, *63*, 197−204.
(111) Nag, K.; Perez-Gil, J.; Cruz, A.; Keough, K. M. Fluorescently Labeled Pulmonary Surfactant Protein C in Spread Phospholipid Monolayers. *Biophys. J.* **1996**, *71*, 246−256.
(112) Amirkhanian, J. D.; Merritt, T. A. The Influence of pH on Surface Properties of Lung Surfactants. *Lung* **1995**, *173*, 243−254.
(113) Papahadjopoulos, D. Surface Properties of Acidic Phospholipids: Interaction of Monolayers and Hydrated Liquid Crystals with Uni- and Bi-Valent Metal Ions. *Biochim. Biophys. Acta, Biomembr.* **1968**, *163*, 240−254.
(114) Teixeira, V. H.; Vila-Viçosa, D.; Baptista, A. M.; Machuqueiro, M. Protonation of DMPC in a Bilayer Environment Using a Linear Response Approximation. *J. Chem. Theory Comput.* **2014**, *10*, 2176−2184.

DOI: 10.1021/acs.jcim.5b00076
J. Chem. Inf. Model. 2015, 55, 2206−2217